

Signatures of sneutrino dark matter in an extension of the CMSSM

Shankha Banerjee¹, Geneviève Bélanger¹, Biswarup Mukhopadhyaya², Pasquale D. Serpico¹

¹*LAPTH, Univ. de Savoie, CNRS, B.P.110, F-74941 Annecy-le-Vieux, France*

²*Regional Centre for Accelerator-based Particle Physics, Harish-Chandra Research Institute, Chhatnag Road, Jhusi, Allahabad 211019, India*

ABSTRACT: Current data (LHC direct searches, Higgs mass, dark matter-related bounds) severely affect the constrained minimal SUSY standard model (CMSSM) with neutralinos as dark matter candidates. But the evidence for neutrino masses coming from oscillations requires extending the SM with at least right-handed neutrinos with a Dirac mass term. In turn, this implies extending the CMSSM with right-handed sneutrino superpartners, a scenario we dub $\tilde{\nu}$ CMSSM. These additional states constitute alternative dark matter candidates of the superWIMP type, produced via the decay of the long-lived next-to-lightest SUSY particle (NLSP). Here we consider the interesting and likely case where the NLSP is a $\tilde{\tau}$: despite the modest extension with respect to the CMSSM this scenario has the distinctive signatures of heavy, stable charged particles. After taking into account the role played by neutrino mass bounds and the specific cosmological bounds from the big bang nucleosynthesis in selecting the viable parameter space, we discuss the excellent discovery prospects for this model at the future runs of the LHC. We show that it is possible to probe $\tilde{\tau}_1$ masses up to 600 GeV at the 14 TeV LHC with $\mathcal{L} = 1100 \text{ fb}^{-1}$ when one considers a pair production of staus with two or more hard jets through all SUSY processes. We also show the complementary discovery prospects from a direct $\tilde{\tau}_1$ pair production, as well as at the new experiment MoEDAL.

Contents

1	Introduction	1
2	Model and constraints	4
3	Bounds from Big Bang Nucleosynthesis	8
4	Results	10
5	Prospects at the LHC	13
5.1	Two $\tilde{\tau}_1$ and at least two hard jets	17
5.2	Two $\tilde{\tau}_1$ tracks	19
5.3	Passive highly-ionizing track detection	21
6	Summary and conclusions	22

1 Introduction

The search for supersymmetry (SUSY) broken around the TeV scale has been so far unsuccessful at the Large Hadron Collider (LHC) [1–3]. This, together with the requirement of having a Higgs boson mass around 125 GeV [4, 5], puts strong pressure on the idea of SUSY as a solution to the naturalness problem [6–8], a situation further exacerbated if one requires the theory to provide a dark matter candidate matching the relic abundance, now determined to exquisite precision [9]. It is no surprise that the simplest (read most economical) version of SUSY theories becomes the first casualty: the constrained minimal SUSY standard model (CMSSM), based on minimal supergravity (mSUGRA) [10] is currently strongly disfavoured [11, 12]. This is due to the rigid links existing in the different sectors of the theory: direct collider bounds push the strongly interacting sector (squarks and gluinos) to heavy scales, but this also translates into heavy sleptons and gauginos, since they are all largely controlled by the universal gaugino ($m_{1/2}$) and scalar (m_0) masses. This not only portrays a dismal picture for collider searches and the naturalness argument, but also spells trouble for the scenario where dark matter (DM) is made of (dominantly bino) neutralinos, since the heavy mass scales suppression of the dominant annihilation cross-sections generically leads to a too large relic abundance. In addition, the option of a higgsino-like DM candidate face constraints from direct searches [13] unless its mass is at the TeV scale. The latter faces naturalness issues since the Higgsino mass parameter μ is determined in terms of scalar masses in this framework, via the electroweak symmetry breaking condition. Such inter-connected nature of the CMSSM parameters, which all evolve from a limited set (m_0 , $m_{1/2}$, A_0 , $\tan\beta$ and the sign of μ), enhances the difficulty

in finding a suitable DM candidate. Coupled with the fact that m_0 and $m_{1/2}$ also affect the Higgs mass(es), all this has caused the CMSSM to run into rough weather [14–18].

The situation, however, can be quite different with a ‘minor’ change in the particle spectrum, which is in fact suggested by an empirical argument. It is known that the MSSM has no built-in mechanism for generating neutrino masses, the evidence for which has grown in the past two decades into an inescapable reality [19–21], for which the 2015 Nobel Prize in Physics has been recently awarded. The most immediate solution to amend the MSSM is to add three right-handed (RH) neutrino superfields, and the corresponding terms in the superpotential, which would lead to their Yukawa interactions. This also implies the simultaneous existence of three right-chiral sneutrinos, one of which could now be the lightest SUSY particle (LSP) and act as potential DM candidate. However, at least for Dirac neutrino masses, the Yukawa interactions are extremely small ($\simeq 10^{-13}$), and any interaction of the right-sneutrino is proportional to this coupling. As a result, the sneutrino LSP never reaches thermal equilibrium, its abundance being determined by the decay of heavier weakly interacting massive particles (WIMPs) rather than by its annihilation into SM particles as in the standard WIMP freeze-out picture. At the same time, the highly suppressed interaction strength automatically allows such a kind of DM candidate to evade the limits coming from direct DM search experiments in underground detectors. The lack of tight restrictions on the DM mass can in principle relax the constraints on the superparticle spectrum in the CMSSM. Hence in such a scenario one can expect different allowed regions in the parameter space than in the standard CMSSM, with correspondingly peculiar cosmological constraints and observable signals at the LHC. The present work is devoted to an investigation in these directions. The collider signatures of this model will differ significantly from the cases where the sneutrino can be a thermal DM either because of a large mixing with other chiral sneutrino states [22–30], or because the sneutrino couples to some new particle [31–33].

It is obvious that the lightest SUSY particle belonging to the CMSSM spectrum, which we shall also loosely call next-to-lightest SUSY particle (NLSP) ¹ is long-lived if its only R -parity conserving ² decay into the LSP is driven by the tiny neutrino Yukawa coupling. In scenarios, where the MSSM scalar masses evolve from a universal m_0 , the NLSP will generally be a neutralino or the lighter stau. Adding the RH sneutrinos will allow to relax the astrophysical and cosmological constraints on scenarios with a neutralino NLSP, however the collider signatures being similar to those of the standard CMSSM we will not consider this class of scenarios. We will rather concentrate on the case where the stau is the lightest sparticle in the MSSM spectrum - a scenario that can only be made viable with the presence of a sneutrino LSP (or a gravitino). Note that the gravitino mass is an arbitrary parameter in the CMSSM, the gravitino could therefore be the LSP, we will not consider this possibility any further as it has been studied in [34–37]. Contrary to the elusive

¹Within the states available in the $\tilde{\nu}$ CMSSM, accounting for the three generation structure, strictly speaking the NLSP is in fact the second lightest sneutrino, almost degenerate with the LSP in what follows.

²The multiplicative conservation of $R = (-1)^{(3B+L+S)}$ —with B , L , and S denoting the baryon number, the lepton number, and the spin of the particle, respectively—ensures that the LSP is stable and a DM candidate.

LSP, it should be noted that the NLSP should satisfy several cosmological constraints. First, since it is a WIMP-like progenitor of the LSP, its thermal relic abundance obtained upon solving the Boltzmann equation for $\tilde{\tau}_1$ is subject to standard constraints, modulo the rescaling by $m_{\tilde{\nu}_R}/m_{\tilde{\tau}_1}$. Secondly, as will be discussed below in detail, the late decay of the stau NLSP may tamper with light element abundances and jeopardise the big bang nucleosynthesis (BBN) predictions. This puts upper limits on its abundance vs. lifetime, leading to constraints on its mass and interaction strengths.

A stau-NLSP that decays into the sneutrino DM candidate consistent with the observed neutrino mass scale will be stable on the distance scale of a collider detector. Therefore, contrary to customary SUSY scenarios with large missing- E_T signatures, these models are characterized by a pair of highly ionising charged tracks that are seen both in the inner tracking chamber and the muon chamber. This has prompted efforts to identify such tracks via time-delay measurements, leading to lower limits on the order of 350 GeV on the masses of stable taus of this kind. In an earlier publication [38], some of us have shown that certain kinematical selection criteria are particularly effective in separating signal and background, especially for relatively low masses of the stable charged particles. These criteria include cuts on the track transverse momenta (p_T), the scalar sum of the p_T 's of all visible particles, and the invariant mass of the pair of the two most highly ionising tracks in any event. It was also demonstrated in [39, 40] that events selected with the help of these criteria could be used to reconstruct certain superparticle masses. Collider signatures with charged tracks are also expected in models with a substantially massive gravitino LSP [41, 42] or with almost degenerate $\tilde{\tau}_1$ -neutralino LSP [43]. In Ref. [44], the reach for the stau NLSP has been studied in the context of the pMSSM.

Compared with earlier investigations [45], this paper presents a number of improvements: first, we update the cosmological constraints which not only include the relic abundance, but also the upper limit on the neutrino mass and, as argued, the BBN constraints. At the same time, we impose LHC null searches performed till now as well as the requirement of obtaining a scalar mass around 125 GeV, in a scenario where the MSSM spectrum follows from the CMSSM postulates. The allowed spectra thus found are subjected to our proposed selection criteria for the 14 TeV run. We identify in this manner (a) the currently viable $\tilde{\nu}$ CMSSM parameter space with $\tilde{\tau}_1$ -NLSP, $\tilde{\nu}_R$ -LSP, and (b) the regions that can be probed at the LHC with gradually accumulating luminosity.

In section 2 we briefly describe the extended CMSSM model and list all the constraints, *viz.* constraints from the relic abundance, from the elemental abundance of ^4He and ^2H and the existing constraints from runs I and II at the LHC. We review the constraints from Big Bang Nucleosynthesis in section 3. We show the existing available parameter space after implementing all the constraints in section 4. In section 5, we discuss few prospective channels through which the available parameter space can be probed via LHC14 in the High luminosity run at 3000 fb^{-1} . Finally we summarise and conclude in section 6, where we also discuss some possible directions for future studies.

2 Model and constraints

In this section we start by discussing the framework and then we will summarise all the existing constraints used in this analysis. Here we consider the MSSM augmented with three generations of RH (s)neutrinos, with a Dirac mass term (implying extremely small Yukawa couplings). This $\tilde{\nu}$ CMSSM model is the simplest extension of the CMSSM which can explain non-zero masses and mixing of the neutrinos. In the present work we consider lepton number conservation, hence the MSSM superpotential is extended by just one term for each family,

$$W_\nu^R = y_\nu \hat{H}_u \hat{L} \hat{\nu}_R^c, \quad (2.1)$$

where y_ν is the neutrino Yukawa coupling, $\hat{L} = (\hat{\nu}_L, \hat{\ell}_L)$ is the left-handed (LH) lepton superfield, $\hat{H}_u = (\hat{H}_u^+, \hat{H}_u^0)$ is the Higgs superfield which gives masses to the $T_3 = +1/2$ fermions and $\hat{\nu}_R$ is the superfield for the RH neutrinos. This superpotential ensures the presence of RH sneutrinos in the particle spectrum. These sneutrinos will have all their couplings proportional to the corresponding neutrino masses. We will consider mainly the case where neutrinos are degenerate and the sneutrino mass term is universal, hence the sneutrinos will be nearly degenerate. We will assume that the lightest sneutrino that might become the LSP is the RH eigenstate of tau-sneutrino.

In this model, after symmetry breaking the neutrinos obtain their masses as

$$m_\nu = \frac{y_\nu}{\sqrt{2}} v \sin \beta, \quad (2.2)$$

where $v \simeq 246.2$ GeV is the vacuum expectation of the SM-like Higgs boson and $\tan \beta = \langle H_u^0 \rangle / \langle H_d^0 \rangle$. While the details of the sneutrino DM scenario described here are sensitive to the matrix structure of the Yukawa couplings, almost all the qualitative features only rely on the smallness of the Yukawa, with their overall size being the key quantitative parameter, determining for instance the very small decay rate of the $\tilde{\tau}_1$ -NLSP. We shall use the currently allowed range of the largest neutrino mass, m_ν^H , as a proxy for the size of the relevant Yukawa coupling. A lower bound on the coupling can be inferred from global fits of the neutrino oscillation parameters to solar, atmospheric, reactor and accelerator neutrino data, which provide at 3σ the range for the largest mass-squared splitting [46],

$$|\Delta m^2| \equiv |m_3^2 - (m_1^2 + m_2^2)/2| = 2.43(2.38) \pm 0.06 \times 10^{-3} \text{ eV}^2, \quad (2.3)$$

where m_i are the three neutrino masses and the number in parenthesis is for the inverted hierarchy scenario ($m_3 < m_1 < m_2$). The heaviest mass (m_ν^H) is thus bounded by

$$m_\nu^H \geq \sqrt{|\Delta m^2|} \simeq 0.049 \text{ eV}, \quad (2.4)$$

with the equality attained only for hierarchical neutrino masses, when it yields

$$(y_\nu^H \sin \beta)_{\min} \simeq 2.8 \times 10^{-13}. \quad (2.5)$$

The upper limit on this Yukawa coupling follows instead from the upper limit on the absolute neutrino mass scale, which is currently dominated by the cosmological bound

on the sum of neutrino masses. The recent combination [9] of Planck temperature (TT) and polarisation (lowP) data with lensing and external data including supernovae, Baryon acoustic oscillation (BAO) and the astrophysical determination of the Hubble constant H_0 yields (see [9] for details)

$$\sum_{i=1}^3 m_i < 0.23 \text{ eV at } 95\% \text{ CL}; \quad (2.6)$$

This upper limit translates—for a quasi-degenerate neutrino mass spectrum—into $m_\nu^H \lesssim 0.077 \text{ eV}$ which implies

$$(y_\nu^H \sin \beta)_{\max} \simeq 4.4 \times 10^{-13}. \quad (2.7)$$

One must note that this number depends to some extent on the number and type of datasets analysed and on the theoretical model assumed for the cosmological fit. The upper limit Eq. (2.6) could be tightened by a factor ~ 2 (see for instance [47]), essentially leading the allowed Yukawa coupling interval to collapse to the value of Eq. (2.5), or relaxed by a similar factor of $\sim 2 \div 3$ (see [9] for details). Given the fast progress in the field of cosmology, we shall present our “fiducial” results for the Yukawa coupling corresponding to Eq. (2.7), but will also show the impact of lowering its value to the one of Eq. (2.5).

In the CMSSM, SUSY breaking is introduced by universal soft terms for the scalars (m_0) and the gauginos ($m_{1/2}$) along with the trilinear couplings A_0 and the bilinear term for the Higgs, B , in the Lagrangian at some high scale. The B parameter and the super-symmetric Higgs mass parameter, μ are determined by the electroweak symmetry breaking conditions (up to the sign of μ). Once the soft SUSY breaking parameters are specified at a high scale ($\mathcal{O}(10^{15}) \text{ GeV}$) and $\tan \beta$ is fixed at the electroweak scale one can determine the masses of all the squarks, sleptons, gauginos as well as the mass parameters of the Higgs sector using the renormalization group equations (RG). In the $\tilde{\nu}$ CMSSM, the RH sneutrino has little impact on the rest of the spectrum, hence the superparticle spectrum almost exactly mimics the one obtained in the CMSSM save for the fact that now the LSP can be the RH sneutrino. Neglecting any inter-family mixing, the additional mass term for the sneutrinos reads

$$-\mathcal{L}_{\text{soft}} \supset M_{\tilde{\nu}_R}^2 |\tilde{\nu}_R|^2 + (y_\nu A_\nu H_u \tilde{L} \tilde{\nu}_R^c + h.c.), \quad (2.8)$$

where A_ν is responsible for the left-right mixing in the scalar mass matrix. It is obtained by the running of the trilinear soft SUSY breaking term, A_0 . Note that we assume a sneutrino mixing that depends on $y_\nu A_\nu$ as is typically the case in SUGRA-inspired scenario where the trilinear soft terms arise from F-terms. From the RG equation solution it is shown in Ref. [48] that at the scale m_Z , A_ν is given by $A_\nu = A_0 - 0.59 m_{1/2}$. The left-right mixing angle of the sneutrino $\tilde{\Theta}$ is given by

$$\tan 2\tilde{\Theta} = \frac{2y_\nu v \sin \beta |\cot \beta \mu - A_\nu|}{m_{\tilde{\nu}_L}^2 - m_{\tilde{\nu}_R}^2}. \quad (2.9)$$

Owing to the fact the neutrino Yukawa couplings are extremely small, the sneutrino mixing can be neglected. We consider the LH and RH sneutrinos as mass eigenstates with

$$m_{\tilde{\nu}_L}^2 = M_L^2 + \frac{1}{2} m_Z^2 \cos 2\beta \quad \text{and} \quad m_{\tilde{\nu}_R}^2 = M_{\tilde{\nu}_R}^2, \quad (2.10)$$

where $M_{\tilde{L}}$ and $M_{\tilde{\nu}_R}$ are the soft scalar masses for the LH sleptons and the RH neutrinos respectively. The right chiral neutrino superfield is different from the remaining fields in MSSM; it has no gauge interaction, and it interacts with MSSM fields only via the Yukawa terms in the superpotential, where again the interaction strengths are very different from those for the other fields, leading to extremely small neutrino masses. All this suggests a somewhat separate status for these superfields, including the possibility of its being actually a member of a hidden sector. In view of all this, one may like to accord a different origin for the right neutrino soft masses, as compared to those arising from m_0 . Keeping this in mind, we will not necessarily require $M_{\tilde{\nu}_R} = m_0$, although we do comment on the consequence of this assumption.

Note that the RG evolution of all the parameters of the CMSSM remain almost unaffected in the $\tilde{\nu}$ CMSSM, with the evolution of the new states being almost negligible: The RH sneutrino mass parameter evolves at one-loop level as [49]

$$\frac{dM_{\tilde{\nu}_R}^2}{dt} = \frac{2}{16\pi^2} y_\nu^2 A_\nu^2. \quad (2.11)$$

Hence, the smallness of the Yukawa coupling ensures that $M_{\tilde{\nu}_R}$ remains basically fixed at its UV value, whereas all the other sfermion masses evolve up at the electroweak scale. It is also worth noting that all three right sneutrinos are similar in nature and, for a universal value of the matrix $M_{\tilde{\nu}_R}$ eigenvalues at high scale, one has a near-degeneracy of three RH sneutrinos, with splittings $\delta M_{\tilde{\nu}_R}^2$ of the order of the neutrino mass splittings δm_ν^2 . Thus the universal GUT scale conditions on the parameters of an R-parity conserving scenario can generate a spectrum where the three RH sneutrinos will be stable (or metastable but very long-lived), leading to different decay chains for supersymmetric particles as compared to those with a neutralino LSP.

To make the discussion more comprehensive, we discuss one important reason for choosing a stau-NLSP [38]. In general one can also have a neutralino or a chargino NLSP as they are the remaining R-odd weakly interacting particles. However, a neutralino NLSP will always end up decaying to a neutrino and a sneutrino leading to a fully invisible final state. Hence the collider signals will be almost exactly the same as for a model with a neutralino LSP. A chargino NLSP can have different signatures through charged tracks. However, it is very difficult to have a model where the lighter chargino (χ_1^\pm) is lighter than the lightest neutralino (χ_1^0), although it can happen at tree-level in specific corners of the MSSM [50]. On the other hand, it is very easy to accommodate a $\tilde{\tau}_1$ -NLSP in the $\tilde{\nu}$ CMSSM scenario, which is thus the case we concentrate on in the following.

The $\tilde{\tau}_1$ -NLSP eventually decays into the RH sneutrinos via $\tilde{\tau}_1 \rightarrow W^{(*)} \tilde{\nu}_R$ (actually all $\tilde{\nu}_R$ states in the degenerate case we are focusing on) driven by the tiny neutrino Yukawa coupling. If we further assume $m_{\tilde{\tau}_1} > m_{\tilde{\nu}_R} + m_W$, the two-body decay width is given by [48]

$$\Gamma_{\tilde{\tau}_1} \simeq \Gamma_{\tilde{\tau}_1 \rightarrow \tilde{\nu}_R W} = \frac{g^2 \tilde{\Theta}^2}{32\pi} |U_{L1}^{(\tilde{\tau}_1)}|^2 \frac{m_{\tilde{\tau}_1}^3}{m_W^2} \left[1 - \frac{2(m_{\tilde{\nu}_R}^2 + m_W^2)}{m_{\tilde{\tau}_1}^2} + \frac{(m_{\tilde{\nu}_R}^2 - m_W^2)^2}{m_{\tilde{\tau}_1}^4} \right]^{3/2}, \quad (2.12)$$

where g is the $SU(2)_L$ gauge coupling constant, m_W is the mass of the W -boson and $U^{(\tilde{\tau}_1)}$ is the mixing matrix of the staus which relate the two mass eigenstates (here $m_{\tilde{\tau}_1} \leq m_{\tilde{\tau}_2}$)

and the gauge eigenstates as

$$\begin{pmatrix} \tilde{\tau}_L \\ \tilde{\tau}_R \end{pmatrix} = U^{(\tilde{\tau})} \begin{pmatrix} \tilde{\tau}_1 \\ \tilde{\tau}_2 \end{pmatrix}, \quad (2.13)$$

and the subscript $L1$ indicates the $(1, 1)^{\text{th}}$ element of this matrix. When $m_{\tilde{\tau}_1} < m_{\tilde{\nu}_R} + m_W$ the two-body decay is kinematically forbidden and the dominant three body decays are $\tilde{\tau}_1 \rightarrow \tilde{\nu}_R \ell \bar{\nu}, \tilde{\nu}_R q \bar{q}'$. The stau lifetime strongly depend on the decay modes and on the mixing in the $\tilde{\nu}$ and $\tilde{\tau}$ sectors, typical lifetimes range from a few seconds to over 10^{11} s.

The lifetime of the NLSP is long enough that its decay occurs well after its freeze-out, yet it has been shown in Ref. [48, 51] that the $\tilde{\nu}_R$ retains all good properties as cold DM, being in particular stable due to R-parity conservation, and evading direct detection constraints due to the suppressed interactions from the tiny Yukawa coupling. The density parameter of $\tilde{\nu}_R$ from the decay of the NLSP after freeze-out is simply given by

$$\Omega_{\tilde{\nu}_R} = \frac{m_{\tilde{\nu}_R}}{m_{\tilde{\tau}_1}} \Omega_{\tilde{\tau}_1}, \quad (2.14)$$

where $\Omega_{\tilde{\tau}_1}$ is the present density parameter of the NLSP assumed stable. In the present work $\Omega_{\tilde{\tau}_1}$ is computed using the code `micrOMEGAs` [52, 53]. Note that in the following we neglect any enhancement in the DM abundance that could come from other production channels, such as heavier sleptons decays (either directly into $\tilde{\nu}_R$ or, more likely, via $\tilde{\tau}_1$). Especially for moderately degenerate slepton mass spectra, these could enhance $\Omega_{\tilde{\nu}_R}$ by an amount that can be estimated at the $\mathcal{O}(10\%)$ level, which should be kept in mind. Recent cosmological data [9] yield

$$\Omega_{\text{DM}} h^2 = 0.1199 \pm 0.0027. \quad (2.15)$$

We shall use Eq. (2.15) as a constraint, requiring that $\Omega_{\tilde{\nu}_R} < \Omega_{\text{DM}}^{\text{max}}$, for which we use the 2σ upper value. In general, we shall find that $\Omega_{\tilde{\nu}_R} < \Omega_{\text{DM}}$, although in some region of parameter space $\Omega_{\tilde{\nu}_R} \simeq \Omega_{\text{DM}}$, *i.e.* the $\tilde{\nu}_R$ produced via $\tilde{\tau}_1$ decay may constitute a sizable (if not dominant) constituent of the DM. Note that this can happen for a range of parameters when the NLSP (which is actually the CMSSM-LSP) is charged, a situation very different from the case where the neutralino constitutes the CMSSM-LSP. A few more particle physics tools are used and constraints are imposed to ensure the phenomenological viability of our model:

- The CMSSM spectrum is generated using SPheno [54, 55].
- The mass of the lightest Higgs is required to be in the range $123 \text{ GeV} < m_{h^0} < 128 \text{ GeV}$, consistent with the Higgs mass measurements from the different channels at the LHC [56] after allowing for a $\simeq 2 \text{ GeV}$ theoretical uncertainty.
- The signal strengths of the SM-like Higgs boson are required to match the experimentally quoted numbers [57, 58]. For this we use the package Lilith [59] which computes the likelihood function and rejects parameter points incompatible with the signal strength measurements.

- We demand that the mass of the long lived $\tilde{\tau}_1 > 340$ GeV, which is the bound obtained by CMS [60, 61] from the run I data for a direct pair production of staus. The bound from ATLAS [62] is slightly weaker, *viz.* $\tilde{\tau}_1 > 289$ GeV.
- We further impose the 2σ bounds from $b \rightarrow s\gamma$ at NLO [63], $B_s \rightarrow \mu^+\mu^-$, [64] and $\bar{B}^+ \rightarrow \tau^+\nu_\tau$ [65], as computed with `micrOMEGAs` [53].
- We demand that $m_{\tilde{g}} > 1.8$ TeV, this value correspond to the the limit obtained from the LHC Run II data [66] that extends on the already stringent bound of Run 1 [67]. Note that this bound refers to the CMSSM and does not apply directly to the $\tilde{\nu}$ CMSSM that we consider here. However, because of the relation between supersymmetric particles masses, the lower bound on the long-lived stau mentioned above forces the gluino to be rather heavy in our model.
- Finally we consider what are perhaps the most important constraints in this study, *i.e.* the constraints on the light nuclei produced in BBN. This constraint is discussed in details in section 3.

3 Bounds from Big Bang Nucleosynthesis

Despite the fact that nuclear binding energies range in the ballpark of several MeV per nucleon, as long as the temperature $T \gg 0.1$ MeV, virtually no nuclear species is present in the early universe, since the high entropy conditions cause the immediate photo-destruction of any bound states that forms. Standard primordial nucleosynthesis (for reviews, see for instance [68, 69]) describes the departure from the early phase of nuclear statistical equilibrium until the synthesis of light nuclei in the cooling plasma is completed, at $T \sim \mathcal{O}(10)$ keV. Since all processes happen at the kinetic equilibrium, in standard BBN the energies available for the nuclear reactions are limited, and the process can be described in a relatively simple and robust way.

When long-lived states are present in the early universe, if their decay injects energetic particles with *visible*³ energy per decay $E_{vis} \gg T$, they can trigger complicated *non-thermal* nuclear processes (non-thermal BBN). Qualitatively, there are two types of processes and constraints. In general, one always expects sizable fractions of energy to be injected in the form of non-thermal photons and electrons (e.m. channels, henceforth simply “photons”): the associated constraints are very strong for lifetimes exceeding $\sim 10^6$ s, see [70] and notably [71] for a recent overview and treatment of these processes including a regime overlooked so far. This constraint however excludes only the long-lifetime tail of the viable $\tilde{\tau}_1$ ’s parameter space, weakening significantly for lower lifetimes and vanishing for injection times below $\sim 10^4$ s. This is due to the fact that e^\pm pair production by energetic photons onto the thermal bath ones is extremely efficient in cutting off the high-energy tail of the photon spectra, with a cutoff energy that increases with decreasing plasma temperature. The cutoff must be larger than the threshold for photodisintegration cross sections in

³This excludes dark byproducts and to a large extent neutrinos.

order for these processes to be relevant, which implies efficient bounds only at sufficiently late times [68].

However, the $\tilde{\tau}_1$'s in the bulk of the parameter space of interest have lifetimes shorter than 10^4 s: for those, the relevant bounds are due to the *hadronic* part of the cascades (with branching ratio B_h) induced by the stau decays, notably via the effects of mesons in altering the weak $n \leftrightarrow p$ equilibrium and of non-thermal nucleons on the nuclear reactions, e.g. via spallations [68]. This dynamics can only be described properly via Monte Carlo simulations, see for instance [72, 73], since some energy-losses are intrinsically stochastic, and using averages in deterministic equations may be inaccurate. Here we base our constraints on the results obtained in [72]. However, we do take into account the newer determinations of the abundances of light nuclei, notably ^2H and ^4He , for which sufficiently precise measurements exist and for which the primordial origin of the bulk of their abundance is not disputed [68, 69]. As explicitly noted in [73] (see its Appendix A), when a single process dominates the production (or destruction) of a given nucleus, a good approximation consists in assuming a linear relation for the change in the number of nuclei with respect to the standard BBN yield vs. the number of decays/particle injected (at any given time). This property is used in our analysis since this “single process dominance” is well satisfied in our scenarios. The ^4He bound relies on its overproduction due to the alteration of the n/p ratio in the early ($t \lesssim 10$ s) BBN phase, with little to no role for the alteration of the nuclear network; the deuterium bound comes essentially from requiring that ^2H is not overproduced via hadro-disintegration of ^4He , see Table IV in [72]. Note also that the bounds reported in [51] and that we want to update are based on the results of Fig. 39 in [72]. For our reference standard computations, we rely on the `ParthENoPE` code (see [68, 74]), which for an adopted baryon to photon ratio of $\eta = 6.1 \times 10^{-10}$ yields best-fit predictions of $Y_p = 0.2463$ and $^2\text{H}/\text{H} = 2.578 \times 10^{-5}$ for ^4He mass fraction and deuterium number density, respectively. It has been recently checked [69] that very similar values (at the permil level) are obtained in an updated version of the Kawano code [75], hence we expect a good agreement of the above figures with the baseline values that had been adopted in [72], which relied on an updated Kawano code.

Between the two curves for ^4He reported in [51], the most relevant one is the constraint relying on the determination [76], denoted as IT. In fact, if we take the 2σ upper limit by summing in quadrature the statistical and systematic error as reported in Eq. (2.4) of [72], the ^4He change leading to the 95% C.L. exclusion in [72] can be estimated as $\Delta Y_p = 0.0066$. The recent determination reported in [69] (see Eq. (7) at zero metallicity) would lead to a two sigma upper limit $Y_p^{\text{max}} \simeq 0.2529$, implying *by accident* exactly the same maximal allowed variation used a decade ago! We conclude that the state-of-the art limit coming from ^4He coincides to a good extent, albeit serendipitously, with the IT curve quoted in [72], which we shall use henceforth.

Concerning deuterium we will consider the “low abundance” bound presented in Ref. [72] as a reference point since, relying on the combination of measurements reported in [77], it uses an abundance $^2\text{H}/\text{H} = 2.78^{+0.44}_{-0.38} \times 10^{-5}$ which is quite close to a more recent determination. This corresponds to an estimated maximal allowed change $\Delta ^2\text{H}/\text{H} \simeq 1.08 \times 10^{-5}$. Based on modern observations, even the conservative ranges used now in

the literature converge to a more restrictive variation, for instance $\Delta^2\text{H}/\text{H} \lesssim 0.9 \times 10^{-5}$ according to [78], or $\Delta^2\text{H}/\text{H} = 0.73 \times 10^{-5}$ based on the compilation in [68], i.e. bounds between 20% and 50% more stringent. If considering the best measurement available $\Delta^2\text{H}/\text{H} = (2.53 \pm 0.04) \times 10^{-5}$ [79] (see also Eq. (8) in [69]) as representative of the state of the art, the largest variation allowed could be as small as $\Delta^2\text{H}/\text{H} \simeq 0.03 \times 10^{-5}$, *i.e.* the room for an exotic effect would have shrank by a factor ~ 36 as compared with the old estimates! Despite this huge improvement, the impact of the deuterium determination on the existing bounds on $\tilde{\tau}_1$'s is only moderate, since the deuterium constraint is a very sharp function of the lifetime, behaving almost like a step function around lifetimes of ~ 100 s. In the following sections, unless otherwise stated, we shall conservatively assume the allowed deuterium interval improved by a mere 20% over the one corresponding to the old “low abundance” determination of Fig. 39 of [72], we call this the conservative constraint. Yet, in order to gauge the impact of possible much higher precision in deuterium observations, we shall also compare those bounds to the constraint coming from the effect of a tightening of the maximal allowed “exotic” deuterium production by a factor 36, corresponding to the most optimistic/aggressive current estimates.

4 Results

In this section we explore the parameter space of the $\tilde{\nu}\text{CMSSM}$ satisfying all constraints listed in the above two sections. The input parameters of the model at GUT scale are varied in the range

$$m_0 < 2500 \text{ GeV} ; \quad m_{1/2} < 2500 \text{ GeV} ; \quad |A_0| < 3000 \text{ GeV} ; \quad (4.1)$$

while at the electroweak scale

$$0 < m_{\tilde{\nu}_R} < m_{\tilde{\tau}_1} ; \quad 5 < \tan \beta < 40 \quad (4.2)$$

and $\text{sign}(\mu) > 0$. Note that in order to be more general we have not fixed the right sneutrino mass at m_0 but rather used its value at the electroweak scale as a free parameter. This could qualitatively be justified since sneutrinos are gauge singlets. In any case we will show the impact of this assumption.

Our benchmark case assumes quasi-degenerate neutrino masses, with $y_\nu = 4.4 \times 10^{-13}$. To show the sensitivity to this value, we shall also present how the results would change for a case with $y_\nu = 2.83 \times 10^{-13}$, loosely inspired to the mass scale associated to a normal hierarchy pattern, but without any flavour structure being imposed. In figure 1, we show the allowed region in the $m_{\tilde{\tau}_1} - m_{\tilde{\nu}_R}$ parameter space, denoted $m_{\text{NLSP}} - m_{\text{LSP}}$. Clearly regions exist where more than 50% of the relic abundance can be accounted for via $m_{\tilde{\nu}_R}$'s. We even find a region in parameter space where more than 80% of the relic abundance can be accounted for, which loosely corresponds to accounting for the totality of the DM after including theoretical uncertainties, for example from higher order effects [80]. Note that the BBN constraint, by imposing an upper limit on the stau lifetime, effectively removes the region of small $m_{\tilde{\tau}_1} - m_{\tilde{\nu}_R}$ mass splitting where the 3-body decay of the stau dominates

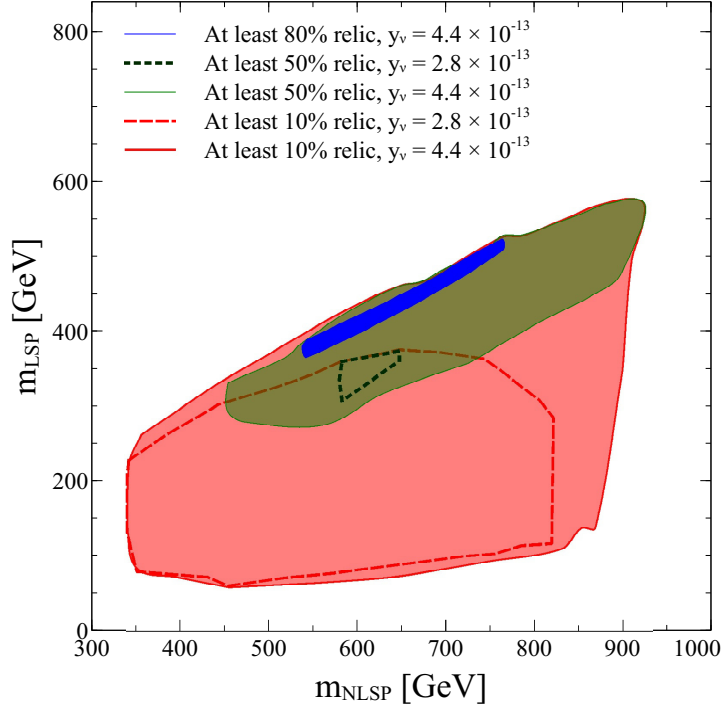


Figure 1. Allowed parameter region showing percentage relic abundance in the $m_{\tilde{\tau}_1} - m_{\tilde{\nu}_R}$ ($m_{\text{NLSP}} - m_{\text{LSP}}$) space for two different values of the Yukawa coupling corresponding to the degenerate and ‘hierarchical’ neutrino masses.

and even some of the region where only 2-body decays occur. Note that the allowed regions shrink when the lower value of the Yukawa coupling is adopted (dashed contour) and no region can be found where $m_{\tilde{\nu}_R}$ ’s contribute 80% or more to the DM. This is because a smaller Yukawa means a smaller sneutrino mixing, leading to a longer lifetime and more severe BBN constraints. Interestingly enough, *the fate of this DM candidate is linked to the sharpness of the cosmological neutrino mass constraints*. A positive detection of the neutrino mass in the degenerate limit, *i.e.* just around the corner, would be compatible with the scenario described in this paper accounting for most if not all of the DM. Should the neutrino mass pattern be constrained to (or detected at) a hierarchical spectrum, at most a sub-leading DM role would be possible for $m_{\tilde{\nu}_R}$ ’s in our scenario.

In figure 2, we show how the parameter region changes once we impose the universality condition on the RH sneutrino mass, more precisely we demand that $|m_{\tilde{\nu}_R} - m_0| < 5$ GeV. This amounts to removing one free parameter of the model. For a given value of $m_{\tilde{\nu}_R}$ we therefore expect a reduced upper bound on the mass of the stau NLSP, even before imposing any constraints, since for a fixed m_0 the range of predicted masses are determined only by the term proportional to $m_{1/2}$ in the RGE. The impact of the BBN constraints is, in both scenarios, to restrict the region at large $m_{\tilde{\tau}_1}$ (and $m_{\tilde{\nu}_L}$). We found however that the upper bound on the mass of the NLSP is much lower ($m_{\tilde{\tau}_1} \approx 600$ GeV) in the

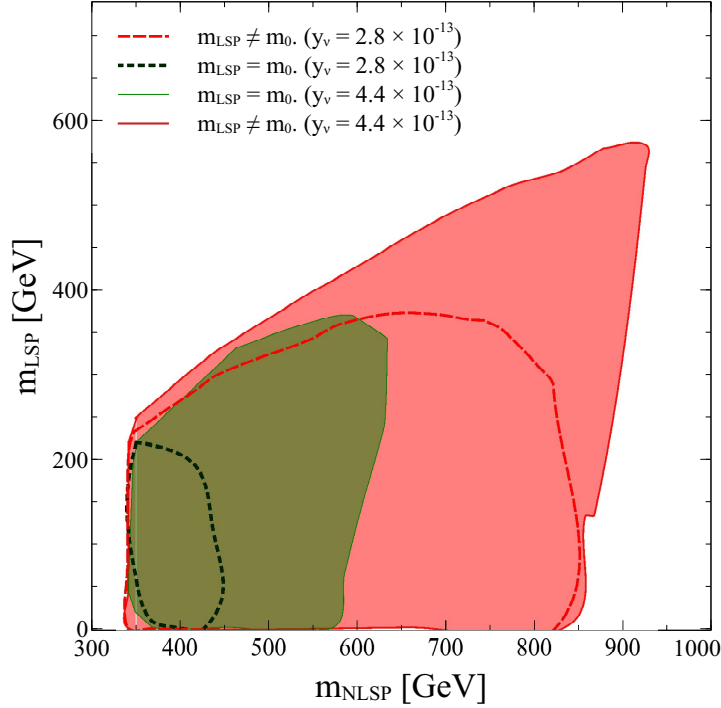


Figure 2. Allowed parameter region showing the change in assuming $m_{\tilde{\nu}_R} = m_0$ in the $m_{\tilde{\tau}_1} - m_{\tilde{\nu}_R}$ ($m_{NLSP} - m_{LSP}$) space for the ‘hierarchical’ (dashed) and degenerate (solid) neutrino masses.

restrictive (“unified”) scenario. The reason is two-fold. First, the sneutrino mixing angle is suppressed for large $m_{\tilde{\nu}_L}$, see Eq. (2.9); this leads to a longer lifetime and thus tighter constraints from $^2\text{H}/\text{H}$. Moreover, we found more points with large mixing in the generic scenario than in the restrictive one. Secondly, the relic density of the NLSP depends on all parameters of the stau sector, and in particular on m_0 , as it enters into the calculation of the stau-annihilation rate. For similar NLSP and LSP masses we found larger values for $\Omega_{\tilde{\tau}_1}$, which implies a larger yield Y_{NLSP} in the unified model, in turn leading to a more stringent constraint from ^4He . As a result, heavier $\tilde{\tau}_1$ ’s are excluded in the more restrictive (“unified”) scenario, but as long as the Yukawa coupling is close enough to the current degenerate upper limit, the reduction of the allowed parameter space is not too dramatic.

To get an idea of the impact of the different bounds in another direction in parameter space, in Fig. 3 we show the allowed region in the $m_0 - m_{1/2}$ plane for the two values of the neutrino Yukawa coupling; here A_0 and $\tan\beta$ vary in the range specified in Eq.s (4.1), (4.2) and $\text{sign}(\mu) > 0$. Note that this allowed parameter space is different from the one obtained in the CMSSM, see for example the result shown by ATLAS with the Run 1 data [67] or [17]. The main difference is that the region at very low m_0 , forbidden in the CMSSM because the LSP is charged, is now re-open. Moreover in the CMSSM the DM relic density imposes the stau and neutralino to be almost degenerate at low m_0 for coannihilation to take place, while in the $\tilde{\nu}$ CMSSM this mechanism is not required and values of m_0 above

the TeV are allowed.

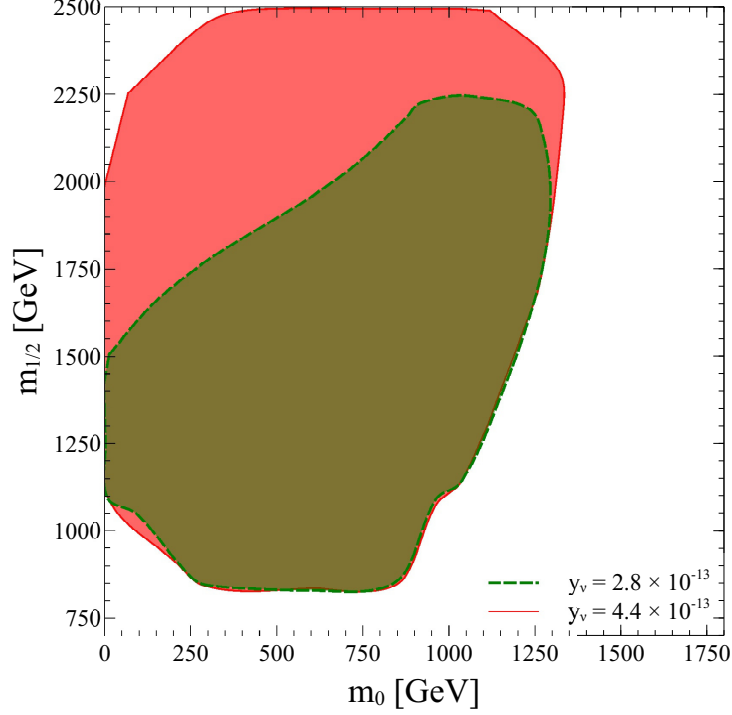


Figure 3. Allowed parameter region in the $m_0 - m_{1/2}$ plane which satisfies all existing collider, low energy, relic and BBN constraints for the ‘hierarchical’ (green) and degenerate (red) neutrino masses. Here we have scanned the parameters as follows: $m_{0,1/2} < 2500$ GeV, $|A_0| < 3000$ GeV, $5 < \tan \beta < 40$, $0 < m_{\tilde{\nu}_R} < m_0$ and $\text{sign}(\mu) > 0$.

Finally, in Fig. 4 we show the impact of BBN constraints from ^4He and $^2\text{H}/\text{H}$ in the relevant parameter space, essentially determined by the lifetime of the long-lived $\tilde{\tau}_1$, denoted τ_{NLSP} , and the “visible energy” $E_{vis} = \frac{m_{\tilde{\tau}_1}^2 + m_W^2 - m_{\tilde{\nu}_R}^2}{2m_{\tilde{\tau}_1}}$, with $B_{had} = 2/3$ corresponding to the hadronic branching fraction of $\tilde{\tau}_1$ for two body decays. The number density to entropy density ratio at $\tilde{\tau}_1$ freeze-out, Y_{NLSP} , is determined by micrOMEGAs.

Note that the main impact of reducing the neutrino Yukawa coupling is to “shift” the lifetime of the $\tilde{\tau}_1$ to longer values, tightening the bounds. The viable region is hence cornered in a small region of the cosmological parameter space, and could be further tightened by an improved neutrino mass limit, and/or an improved ^4He determination. Note that the ^2H constraining power is basically saturated, with a determination more aggressive by a factor 36 only improving the lifetime bound by $\sim 20\%$ or so.

5 Prospects at the LHC

In this section we study the discovery prospects of the $\tilde{\tau}_1$ -NLSP at the future runs of the LHC. We focus on the following channels, *viz.*

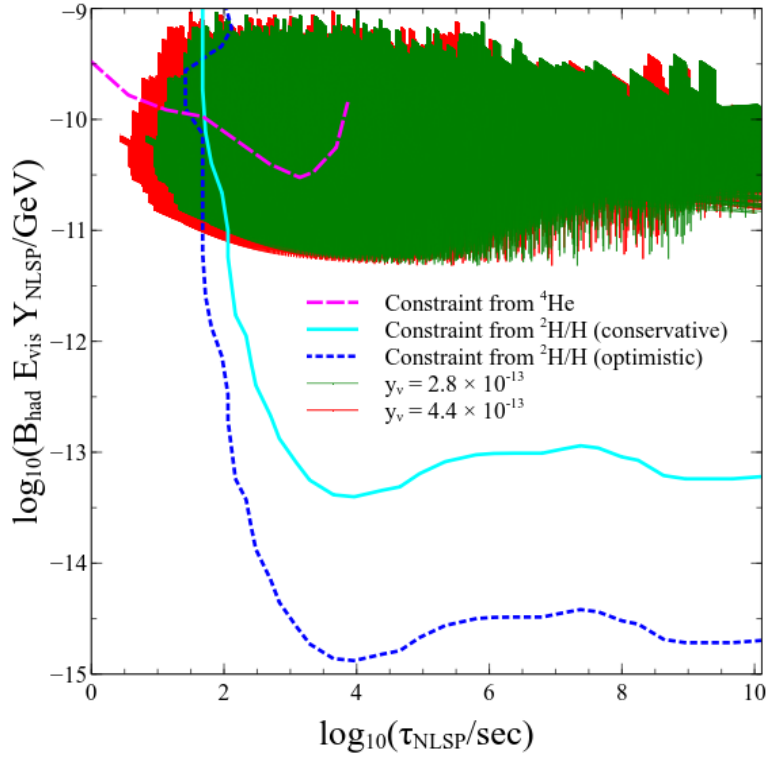


Figure 4. Allowed parameter region (below the ^4He line and to the left of the $^2\text{H}/\text{H}$ line) in the lifetime-injected hadronic energy plane which satisfies all existing collider, low energy, relic and BBN constraints for the ‘hierarchical’ (green) and degenerate (red) neutrino masses. The two curves denote the constraint from ^4He (magenta dashed) and from $^2\text{H}/\text{H}$ (cyan solid) abundance. The dotted (blue) curve represents the impact of assuming a more tightening $^2\text{H}/\text{H}$ determination.

- $2\tilde{\tau}_1 + N$ hard jets ($N \geq 2$),
- $2\tilde{\tau}_1$ (two stable charged tracks),
- passive detection of highly-ionizing (slow) particles,

described in Sec. 5.1, Sec. 5.2, and Sec. 5.3, respectively. Out of the allowed parameter region determined in the previous section, we take four benchmark points with increasing $\tilde{\tau}_1$ mass and show their discovery prospect at the 14 TeV run of the LHC with an integrated luminosity up to 3000 fb^{-1} . The four benchmark points are listed in Table 1.

For these benchmarks, the low energy spectrum follows the general trend,

$$m_{\tilde{\nu}_R} < m_{\tilde{\tau}_1} < m_{\chi_1^0} < m_{\tilde{e}_1, \tilde{\mu}_1} < \dots < m_{\tilde{g}}$$

suggesting that all superparticle productions at the LHC would finally end up decaying to the sneutrino-LSP. However, we must note that the lifetime of the $\tilde{\tau}_1$ -NLSP varies roughly between a few seconds to a little more than three minutes for the allowed parameter space. Thus these particles will decay only outside the detector. Within the general

Parameter	Benchmark 1	Benchmark 2	Benchmark 3	Benchmark 4
m_0	99,	284,	690	944
$m_{1/2}$	1048	961	1369	1661
A_0	-1897	-2115	-206,	- 2175
$\tan \beta$	10.35	11.18	33.49	38.67
μ	1620	1590	1923	2202
$m_{\tilde{e}_L}, m_{\tilde{\mu}_L}$	705	701	1138	1443
$m_{\tilde{e}_R}, m_{\tilde{\mu}_R}$	408	460	859	1127
$m_{\tilde{\nu}_{e_L}}, m_{\tilde{\nu}_{\mu_L}}$	700	697	1134	1440
$m_{\tilde{\nu}_{\tau_L}}$	687	679	1011	1275
$m_{\tilde{\tau}_1}$	357	399	442	598
$m_{\tilde{\tau}_2}$	694	687	1024	1286
$m_{\chi_1^0}$	447	409	594	727
$m_{\chi_2^0}$	848	778	1121	1366
$m_{\chi_1^\pm}$	848	778	1121	1366
$m_{\tilde{g}}$	2295	2121	2956	3543
$m_{\tilde{u}_L}, m_{\tilde{c}_L}$	2088	1947	2754	3321
$m_{\tilde{u}_R}, m_{\tilde{c}_R}$	2000	1868	2642	3185
$m_{\tilde{d}_L}, m_{\tilde{s}_L}$	2089	1948	2755	3322
$m_{\tilde{d}_R}, m_{\tilde{s}_R}$	1991	1860	2629	3170
$m_{\tilde{t}_1}$	1385	1210	1914	2358
$m_{\tilde{t}_2}$	1849	1698	2351	2819
$m_{\tilde{b}_1}$	1814	1659	2316	2783
$m_{\tilde{b}_2}$	1970	1834	2423	2875
m_{h^0}	124	124	125	126
m_{A^0}	1739	1699	1764	1924

Table 1. Benchmark points for studying the discovery prospects of the $\tilde{\tau}_1$ -NLSP in the $\tilde{\nu}$ CMSSM framework with a RH sneutrino LSP. All the superparticle masses and dimensionful input parameters are shown in GeV. The $\tilde{\nu}_{i_R}$ masses are not shown in the table as the exact value is not important for the collider phenomenology provided $m_{\tilde{\nu}_{i_R}} < m_{\tilde{\tau}_1}$. The top mass is fixed at 173.1 GeV and has been used for the running of the parameters.

purpose ATLAS and CMS detectors, characteristic signatures consist of charged tracks with large transverse momenta. This is in contrast with the standard SUSY signals where the signature involves a substantial amount of missing transverse momenta. Thus, the “stable” $\tilde{\tau}_1$ will behave just like a *slow* muon, *i.e.* their velocity $\beta = p/E$ is appreciably lower than 1, implying that they will have high specific ionisation. Many existing studies in the literature capitalise on the ionisation properties and the time of flight measurements of these particles and distinguishes them from the muons [81–87]. There is another approach of separating the signal from the backgrounds by looking at certain kinematic distributions [38] and giving hard cuts on these. In this work, we compare the two approaches for the four

benchmark points listed above. We also briefly mention an unconventional passive search strategy fully relying on this property.

Before we start discussing the analysis strategy, we comment on the mass measurement strategy of these long lived charged particles using the time of flight measurements [88]. When the staus are pair produced, a majority of them have a high velocity. We show the velocity distribution for the third benchmark point in Fig. 5 for stau pair production. This velocity distribution can also be obtained from the time-of-flight measurement in the muon detector system. Combining this with the measured momentum in the same system gives the mass of the particle using the relation

$$m = p/\beta\gamma, \quad (5.1)$$

where γ is the Lorentz factor. The details of this measurement technique can be found in Refs. [62, 88]. Here, we follow a fairly simple-minded approach. Instead of taking the mass of the $\tilde{\tau}_1$ at its fixed value obtained from the SUSY spectrum, we smear its mass as a gaussian with a standard deviation of 5 GeV which is roughly of what is obtained in Ref. [88] considering the uncertainty from the time-of-flight measurements. In doing so, we generate a gaussian random number with its mean as the value of $m_{\tilde{\tau}_1}$ obtained from the SUSY-spectrum and a standard deviation of 5 GeV. We use the Box-Muller transform in generating the gaussian random numbers.

It is also important to comment on the velocity distribution of the muon which is the single most important candidate for our backgrounds. Because we consider β to be an important observable, it is essential to obtain a realistic velocity distribution for the muons. However this is very difficult to mimic from fast detector simulations. Thus, we again refer to the experiments. The velocity distribution of the muons from a combined measurement of the calorimeter and the muon spectrometer has a small spread with a mean value of $\bar{\beta} = 0.999c$ and a standard deviation of $\sigma_\beta = 0.024c$, see Fig. 1 (right) in Ref. [62]. Hence, in our analysis we generate a gaussian random number with these parameters and then impose the cuts on β accordingly. We must note in passing that in BP1 the RH selectron and smuon states are lighter than χ_1^0 . In such cases, the neutralino can decay into $\tilde{e}e(\tilde{\mu}\mu)$. The decays of the charged slepton to the lighter sneutrino state of the first two families are highly suppressed by the small Yukawa couplings, as is the case for the $\tilde{\tau}_1$ -NLSP. However the competing three body decay via a virtual neutralino into the $\tilde{\tau}_1\tau e(\mu)$ or $\tilde{\nu}_\tau\tau\nu_e(\nu_\mu)$ as the final state particles will prevent the selectrons (smuons) from being long-lived. These can however give additional events with $\tilde{\tau}_1$ -tracks. In the analysis below we will not consider the direct production of selectrons and smuons, this process was studied in [38].

In the next two subsections, we discuss the two proposed final states and investigate the discovery prospects of the long-lived $\tilde{\tau}_1$ s. We compute the statistical significance using the standard formula

$$\mathcal{S} = \frac{N_S}{\sqrt{N_S + N_B}}, \quad (5.2)$$

where N_S and N_B are respectively the number of signal and background events passing the selection cuts.

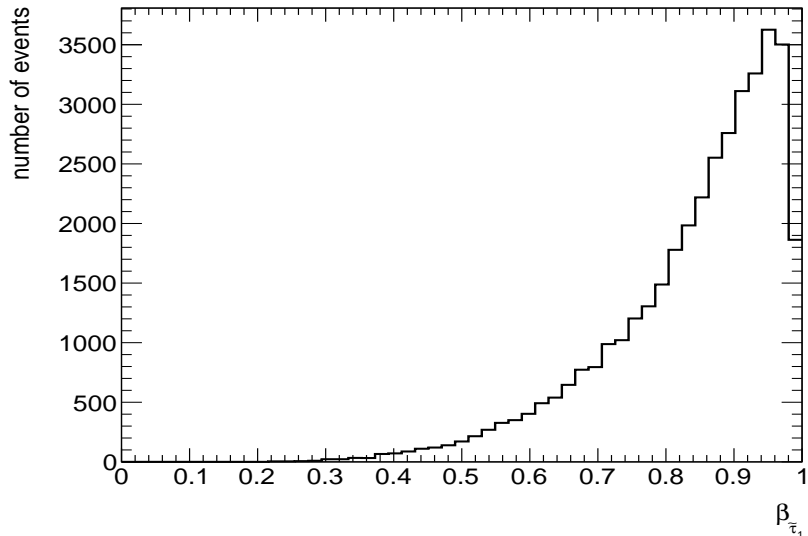


Figure 5. Velocity distribution of the $\tilde{\tau}_1$ -NLSP for benchmark point 3. The mean velocity is $\sim 0.84c$ with an root-mean-square of $\sim 0.13c$.

5.1 Two $\tilde{\tau}_1$ and at least two hard jets

To perform our analysis, we generate the SUSY-spectra using **SPheno** [54, 55]. The output SLHA [89] files are fed into the **MadGraph5 aMC@NLO** [90] program to generate the signal events. The showering and hadronisation is done using **Pythia 6** [91]. Finally the detector simulation is done in the **Delphes 3** [92] framework⁴. In order to decay the χ_1^0 in **Pythia**, we had to modify the main code slightly since the lightest neutralino is by default considered to be the LSP. For the signal generation, the parton distribution functions have been evaluated at $Q = 2m_{\tilde{\tau}_1}$ using **CTEQ6L1** [93]. The renormalisation and factorisation scales are set as

$$\mu_R = Q = \mu_F \quad (5.3)$$

The jets have been formed using the anti- k_t jet clustering algorithm [94] in the **FASTJET** framework [95] with the R parameter set equal to 0.6. The signal cross-sections have been rescaled by their next-to leading order (NLO) k -factors using **Prospino 2** [96]. We generate the signal samples together in **MadGraph** which also gives the cross-sections in the separate channels like squark-squark, squark-gluino and gluino-gluino production. We then compute the k -factors for each of these using **Prospino** and computed the effective k -factor by weighting with the cross-sections in the individual channels.

Since stable staus appear in the SUSY decay chains, the main contribution to this channel comes from squark pair production (sample Feynman diagrams are shown in Fig. 6). The production of one or two gluinos are suppressed relative to the squarks due to the higher

⁴We thank Pavel Demin, Shilpi Jain and Michele Selvaggi for technical help in implementing the $\tilde{\tau}_1$ s as stable charged tracks in the **Delphes 3** framework.

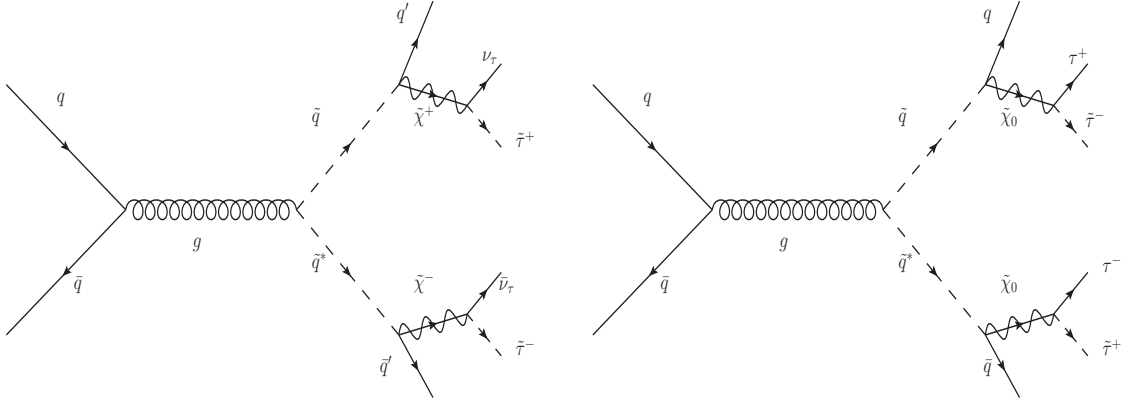


Figure 6. Sample Feynman diagrams showing a pair production of \tilde{t}_1 s with additional jets and \cancel{E}_T or jets and leptons.

mass of the gluino, see Table 1, and the fact that for such high masses the gluon PDF's are small. For this channel the dominant backgrounds are : $t\bar{t}$ (computed at N³LO [97]) and the Drell Yan production of $\mu\mu(\tau\tau)$ + jets (computed at NNLO [98]). For the latter, we take a matched sample, matched up to 3 jets using the MLM ME-PS matching scheme [99]. Besides these, the other contributions to the backgrounds come from W^+W^- , WZ and ZZ and are computed at NLO [100]. Here we take a similar approach as considered in Ref. [38]. Instead of considering the velocity of the stable staus, we consider hard kinematical cuts, specifically

- $p_T^{\mu_{1,2}} > 200 \text{ GeV}$, $|y(\mu_{1,2})| < 2.4$,
- $p_T^{j_{1,2}} > 200 \text{ GeV}$, $|\eta(j_{1,2})| < 5.0$,
- $\sum |p_T^{vis.}| > 1000 \text{ GeV}$,
- $\Delta R(\mu_1, \mu_2) > 0.2$,
- $\Delta R(j, j) > 0.4$,
- $\Delta R(\mu, j) > 0.4$,
- $M_{\mu_1, \mu_2} > 1000 \text{ GeV}$,

where the subscripts 1 and 2 refer to the hardest or the second hardest object when ordered by p_T , and p_T^μ generically refers to the track, be it due to the \tilde{t}_1 signal or the background muons. These cuts have a dramatic effect in removing the backgrounds almost completely. To perform the analysis, we generated a statistically significant number of events such that we are sure of the number of events after the cuts. With the above cuts, we end up with 0 events for WZ + jets and ZZ + jets. In Table 2 we show the luminosity required to reach

a 5σ statistical significance for stable staus for each of the benchmarks. The small number of background events surviving the cuts scales with the luminosity considered for each point. Note that the lower luminosity required for BP2 as compared to BP1 is linked to the fact that the coloured states are lighter for BP2.

Benchmark point	\mathcal{L} for 5σ [fb^{-1}]	N_S	N_B	N_S/N_B
BP1	9.10	25.26	0.35	72.17
BP2	2.45	25.19	0.09	265.2
BP3	68.50	27.42	2.67	10.27
BP4	1100	47.59	42.87	1.11

Table 2. The luminosity required in order to attain a 5σ statistical significance for stable staus for the four benchmarks. The number of signal and background events as well as the ratio N_S/N_B after the selection cuts for that particular luminosity is also displayed.

From these results we conclude that it is fairly simple to probe collider stable staus with masses $\lesssim 400$ GeV (BP1 and BP2) in the early runs of the 14 TeV LHC. Moreover, we estimate with a simple rescaling of the LO cross sections from 14 TeV to 13 TeV, that a 5σ significance is also reachable with the 13 TeV Run with luminosities of roughly 15 (4) fb^{-1} for BP1 (BP2). For larger stau masses (linked with heavier coloured states in our model) one gradually requires larger integrated luminosity: $\mathcal{L} = 1000 \text{ fb}^{-1}$ allows to probe masses up to 580 GeV, with the full integrated luminosity $\mathcal{L} = 3000 \text{ fb}^{-1}$, the mass reach can be extended to roughly 600 GeV, thus allowing to cover a significant fraction of the currently allowed parameter space.

5.2 Two $\tilde{\tau}_1$ tracks

Here, we study the discovery prospects of directly produced $\tilde{\tau}_1$ pairs. This channel suffers from a smaller production cross section as compared to the previous one (electroweak production as compared to strong production) but presents the advantage of being fairly model independent: This channel can also be used beyond the $\tilde{\nu}$ CMSSM framework when the coloured states are too heavy to be produced at a significant rate. Moreover we can directly use the constraints already set by CMS and ATLAS from the run I data, i.e. a lower bound on the $\tilde{\tau}_1$ mass of 289 GeV and 340 GeV from ATLAS [62] and CMS [60, 61], respectively. These bounds are from the tracker plus time-of-flight measurements. CMS quotes a much relaxed lower bound on the $\tilde{\tau}_1$ mass at 190 GeV from the tracker measurement alone. CMS has also quoted the bound from the 13 TeV run and it is weaker than its 8 TeV counterpart, *viz.* $m_{\tilde{\tau}_1} > 230$ GeV. However, we do not consider this bound and take the more stringent one because the 13 TeV run till now has a significantly small integrated luminosity.

Let us also stress that we have used the Drell-Yan plus $b\bar{b}$ initiated production for the $\tilde{\tau}_1$ pairs in obtaining the final results. It is mentioned in Ref. [101] that the gluon fusion initiated processes can enhance the cross-sections by an order of magnitude. However, this statement holds for $\tilde{\tau}_1$ masses below 250 GeV, with the maximum effect achieved when $100 \text{ GeV} < m_{\tilde{\tau}_1} < 200 \text{ GeV}$. However, in our case the stau is always heavier than 340 GeV. We

Cut on	Cut set A	Cut set B	Cut set C
β	> 0.85	—	< 0.95
$p_T^{\mu_{1,2}}$	$> 200 \text{ GeV}$	$> 200 \text{ GeV}$	$> 70 \text{ GeV}$
$\sum p_T^{vis.} $	$> 700 \text{ GeV}$	$> 500 \text{ GeV}$	—
$ y(\mu_{1,2}) $	< 2.4	< 2.4	< 2.5
M_{μ_1, μ_2}	$> 1200 \text{ GeV}$	$> 1000 \text{ GeV}$	—
$\Delta R(\mu_1, \mu_2)$	> 0.2	> 0.2	—
$\Delta R(\mu, j)$	> 0.4	> 0.4	—
$\Delta R(j, j)$	> 0.4	> 0.4	—

Table 3. The three sets of selection cuts applied in the $\tilde{\tau}_1$ pair analysis. Set C resembles the set of cuts of the ATLAS analysis [62].

find that with an increase in the masses of the particles in the loop, *viz.* the squarks, we have decoupling and this does not lead to any contribution from such loops: we checked explicitly by using MadGraph5 aMC@NLO that at LO, the gluon initiated processes have contributions of the order of $\mathcal{O}(10^{-9} - 10^{-8})$ fb.

For this particular channel the most dominant background is a pair of muons. We generate pairs of muons as well as pairs of taus (which can also lead to a two-muons final state) using MadGraph5 aMC@NLO and use the same procedure for the detector analysis as for the signal. Here we also fold in the next-to-next-to leading order (NNLO) k -factor [98]. We also consider the subdominant backgrounds, *viz.* $t\bar{t}$ and diboson pairs (WW, WZ and ZZ) computed respectively at N³LO [97] and NLO [100].⁵ We use the following basic trigger cuts for our analysis,

- $p_T^\mu > 70 \text{ GeV}$,
- $|\eta(\mu)| < 2.5$,
- $\Delta R(\mu\mu) > 0.4$.

These same cuts have been applied to the $\tilde{\tau}_1$ tracks in the detector analysis because of our inability to generate the samples with such trigger cuts at the generator level using MadGraph. After this we used three sets of selection cuts to see which fares better in terms of the significance. In table 3, we list down the selection cuts in details. The cut set C resembles the one used by ATLAS [62].

The hard p_T cuts are extremely efficient in removing a significant amount of the backgrounds. However, the Cut set C proves to be one of the most efficient ones because the muon velocity distribution peaks roughly around unity with a very small spread⁶. The number of signal and background events and the significances for an integrated luminosity

⁵For low p_T cuts ($p_T \sim 15 \text{ GeV}$), muons from b - and c -decays can have substantial rates [41]. But because we impose a high p_T cut on the muons (see Table 3), and we also require a jet-muon isolation cut, these backgrounds become negligible. Hence we do not explicitly include these backgrounds in our analysis.

⁶Note that Ref. [41] uses slightly different sets of selection cuts including $0.6 < \beta < 0.9$. We have restricted ourselves to weaker cuts on β .

of 3000 fb^{-1} are listed in Table 4, showing that more than 5σ significance can be reached for all points but BP4 with Cut set C or B. With Set A, especially due to the lower bound on β and also to the more stringent cuts on p_T and on the invariant mass, a much larger fraction of the signal is suppressed, leading to smaller significance even though the background is also more suppressed. Note in addition that the reach on $m_{\tilde{\tau}}$ could be extended by requiring a tighter cut on β . Choosing $\beta < 0.8$ as per CMS [60,61], we get statistical significances of 4.7σ and 3.0σ for $m_{\tilde{\tau}} = 700, 800 \text{ GeV}$ respectively. This hard cut on β renders the background vanishingly small: even by including the spread in the muon β distribution from ATLAS [62], we hardly get any background events which pass $\beta < 0.8$.

Cut set	Benchmark point	N_S	N_B	N_S/N_B	\mathcal{S}
A	BP1	526	5684	0.09	6.7
	BP2	358		0.06	4.6
	BP3	258		0.05	3.3
	BP4	47		0.01	0.6
B	BP1	1337	12772	0.10	11.3
	BP2	1069		0.08	8.9
	BP3	826		0.06	7.0
	BP4	232		0.02	2.0
C	BP1	1543	3481	0.44	21.8
	BP2	1014		0.29	15.1
	BP3	715		0.21	11.0
	BP4	211		0.06	3.5

Table 4. Table showing the number of signal and background events after the selection cuts for the three sets of selection cuts, the ratio N_S/N_B and the statistical significance \mathcal{S} . The integrated luminosity used to compute these numbers is 3000 fb^{-1} .

5.3 Passive highly-ionizing track detection

An unconventional search strategy is also possible at the new and largely passive detector MoEDAL [102], mostly comprised of an array of nuclear track detector stacks surrounding the intersection region at Point 8 on the LHC ring, which is sensitive to highly-ionizing particles (a further trapping array is only suitable for very long-lived particle, beyond the regime of interest of our model). This search does not require any trigger and in principle even one detected event would be enough, albeit multiple events would be needed for a robust discovery. The only major condition for sensitivity to the produced $\tilde{\tau}_1$ is that the ionizing particle has a velocity $\beta \leq 0.2$. For illustrative purposes we report in Tab. 5 the numbers of events with $\beta \leq 0.2$ expected for $\mathcal{L} = 3000 \text{ fb}^{-1}$ after imposing that the track has $p_T^\mu > 5 \text{ GeV}$. More detailed full detector simulations are required to be more quantitative but it is already clear that when the staus are produced from decays of coloured particles, there exists a possibility of an independent discovery via this complementary channel for all our benchmarks.

Benchmark point	Cascade (Sec. 5.1)	Direct (Sec. 5.2)
BP1	45	2.5
BP2	296	1.5
BP3	24	1.1
BP4	6	0.5

Table 5. Number of $\tilde{\tau}_1$'s with $\beta \leq 0.2$ potentially detectable by MoEDAL assuming an integrated luminosity of $\mathcal{L} = 3000 \text{ fb}^{-1}$, for the four benchmarks and the two production mechanisms discussed in the text.

6 Summary and conclusions

In this study, we have discussed the prospects of the revival of the CMSSM through one of the simplest extensions, *viz.* through the addition of three families of right handed (s)neutrinos, the $\tilde{\nu}$ CMSSM. We showed that in a sufficient portion of the parameter space the right handed sneutrino might become the LSP and by contributing to the relic abundance it can become a potential cold dark matter candidate. In our study, we focused on an R -parity conserving scenario where the $\tilde{\tau}_1$ -NLSP can be long lived, such that its decay occurs well after its freeze-out. We further imposed all the available constraints, from the Higgs and flavour sector, from SUSY searches at colliders, from neutrino masses and most importantly the BBN constraints on the elemental abundance of ^4He and ^2H . The latter is particularly important in excluding virtually all parameters leading to stau lifetimes beyond a few minutes, which would alter too much the primordial yields via the cascades induced by the $\tilde{\tau}_1$ decay byproducts. After imposing all these constraints, one is left with regions where m_0 and $m_{1/2}$ can range up to 1.4 TeV and ~ 2.5 TeV respectively. One also sees that on demanding more contribution to the relic, the parameter region shrinks. Only a very narrow region remains when demanding that the sneutrino contributes to more than 80% of the dark matter, and this is also very sensitive to the actual value of the neutrino mass scale. For instance, a non-degenerate neutrino mass spectrum, either in the case of normal or inverted mass hierarchy, would imply that the sneutrinos can at most contribute at a subleading level, $\mathcal{O}(10\%)$, to the relic abundance.

Finally we study the prospects of observing such long-lived staus at the recent/future runs of the LHC with three strategies, *viz.*

- From the cascade decays of the production of squark pairs, gluino pairs and pairs of squark and gluino, we find significant mismatch of the kinematic distributions of the signal and the backgrounds. We apply hard cuts on the p_T of the stable tracks (which fake “heavy” muons) and the jets. Furthermore, from the time of flight measurements and the measurement of the velocity of such particles, one can indirectly measure the masses of the staus. We find that a hard cut on the total visible transverse momentum and on the invariant mass of the pair of stable tracks kills all the backgrounds. It is possible to observe such a long-lived stau of mass around 400 GeV at 5σ from the 13 TeV run with an approximate integrated luminosity of 4 fb^{-1} and that a high luminosity run at 14 TeV would probe stable staus as heavy as 600 GeV. The only

drawback of this otherwise promising search is its model dependence, since it relies on the mass of the gluino and the squarks.

- We further show the discovery prospects of a stau when they are directly pair produced. We find that one needs much higher luminosities to potentially discover the staus from this channel, which however presents the advantage of being fairly model independent. With the current set of cuts from ATLAS, a stau of mass around 400 GeV can be discovered with a 14 TeV run at 300 fb^{-1} .
- We briefly discussed the perspective of an additional discovery opportunity at the unconventional MoEDAL passive detector, sensitive to highly-ionizing (slow) tracks. Despite the fact that no detailed simulations are currently available, the number of slow events expected in the high-luminosity run is encouragingly high that a discovery should be within reach in a significant fraction of the parameter space.

To conclude, let us express a few general remarks. It is interesting that a minor modification to the CMSSM (in this case demanded by the empirical evidence for neutrino masses) leads to major phenomenological changes and hence in the appropriate search strategies at colliders. Even though supersymmetry is being pushed to the backseat by every new experimental set of data from the LHC, this qualitative lesson may stay true and apply to a number of alternative scenarios, when moving beyond minimal models. This certainly motivates one to pursue further in devising more involved search techniques like the one sketched in our study. A second consideration concerns the deep links existing between neutrino physics, early universe cosmology (dark matter, BBN) and collider searches: the $\tilde{\nu}$ CMSSM model discussed here is a remarkable illustration of these tight relations, to the point that for instance a neutrino mass measurement at a factor two below current upper limits would rule out a dominant DM role of our sneutrino candidates. Finally, there are other interesting perspectives concerning cosmological and astrophysical consequence of such a kind of DM candidate. One further possibility for diagnostics relies on the fact that sneutrinos are not really “cold” dark matter candidates: Due to the recoil acquired in the decay they may have a sizable kinetic energy. This possibly leads to other observables, like a suppression of small scale cosmic structures due to their free-streaming. Several of these consequences have been explored for other “superWIMP” candidates (see [34] and refs. to it) and we will not repeat them here. On the other hand, our DM candidate has a very peculiar feature, being possibly constituted by a mixture of three almost degenerate sneutrino states. Two of the three states are very long-lived but can decay e.g. via $\tilde{\nu}_2 \rightarrow \tilde{\nu}_1 \nu_\alpha \bar{\nu}_\alpha$. We have not explored here the associated phenomenology, since it crucially depends on the mass matrix pattern of the right-handed sneutrinos. It is possible that some interesting cosmological or astrophysical consequences may follow. This is a further point deserving investigation, notably if forthcoming data should comfort the viability of the model discussed in this article.

Acknowledgments

We thank Bobby Acharya and James Pinfold for useful exchange on the MoEDAL potential. We thank Daniele Barducci, Sanjoy Biswas, Arghya Choudhury, Pavel Demin, Diego Guadagnoli, Shilpi Jain, Olivier Mattelaer, Subhadeep Mondal, Satyanarayan Mukhopadhyay, Emanuele Re and Michele Selvaggi for helpful discussions or technical help at various stages of this work. This work is supported by the “Investissements d’avenir, Labex ENIGMASS”, by the French ANR, Project DMAstro-LHC, ANR-12-BS05-006 and the Indo French LIA THEP (Theoretical High Energy Physics) of the CNRS. The work of BM is partially supported by funding available from the Department of Atomic Energy, Government of India, for the Regional Centre for Accelerator-based Particle Physics (RECAPP), Harish-Chandra Research Institute.

References

- [1] Georges Aad et al. Search for new phenomena in final states with large jet multiplicities and missing transverse momentum with ATLAS using $\sqrt{s} = 13$ TeV proton–proton collisions. 2016.
- [2] Vardan Khachatryan et al. Search for supersymmetry in the multijet and missing transverse momentum final state in pp collisions at 13 TeV. 2016.
- [3] Georges Aad et al. Summary of the ATLAS experiments sensitivity to supersymmetry after LHC Run 1 – interpreted in the phenomenological MSSM. *JHEP*, 10:134, 2015. doi: 10.1007/JHEP10(2015)134.
- [4] Georges Aad et al. Observation of a new particle in the search for the Standard Model Higgs boson with the ATLAS detector at the LHC. *Phys. Lett.*, B716:1–29, 2012. doi: 10.1016/j.physletb.2012.08.020.
- [5] Serguei Chatrchyan et al. Observation of a new boson at a mass of 125 GeV with the CMS experiment at the LHC. *Phys. Lett.*, B716:30–61, 2012. doi: 10.1016/j.physletb.2012.08.021.
- [6] Riccardo Barbieri and G. F. Giudice. Upper Bounds on Supersymmetric Particle Masses. *Nucl. Phys.*, B306:63, 1988. doi: 10.1016/0550-3213(88)90171-X.
- [7] B. de Carlos and J. A. Casas. One loop analysis of the electroweak breaking in supersymmetric models and the fine tuning problem. *Phys. Lett.*, B309:320–328, 1993. doi: 10.1016/0370-2693(93)90940-J.
- [8] Lawrence J. Hall, David Pinner, and Joshua T. Ruderman. A Natural SUSY Higgs Near 126 GeV. *JHEP*, 04:131, 2012. doi: 10.1007/JHEP04(2012)131.
- [9] P. A. R. Ade et al. Planck 2015 results. XIII. Cosmological parameters. 2015.
- [10] Ali H. Chamseddine, Richard L. Arnowitt, and Pran Nath. Locally Supersymmetric Grand Unification. *Phys. Rev. Lett.*, 49:970, 1982. doi: 10.1103/PhysRevLett.49.970.
- [11] Howard Baer, Vernon Barger, Peisi Huang, Dan Mickelson, Azar Mustafayev, and Xerxes Tata. Post-LHC7 fine-tuning in the minimal supergravity/CMSSM model with a 125 GeV Higgs boson. *Phys. Rev.*, D87(3):035017, 2013. doi: 10.1103/PhysRevD.87.035017.

- [12] Dumitru M. Ghilencea, Hyun Min Lee, and Myeonghun Park. Tuning supersymmetric models at the LHC: A comparative analysis at two-loop level. *JHEP*, 07:046, 2012. doi: 10.1007/JHEP07(2012)046.
- [13] D. S. Akerib et al. Improved WIMP scattering limits from the LUX experiment. 2015.
- [14] C. Stenge, G. Bertone, F. Feroz, M. Fornasa, R. Ruiz de Austri, and R. Trotta. Global Fits of the cMSSM and NUHM including the LHC Higgs discovery and new XENON100 constraints. *JCAP*, 1304:013, 2013. doi: 10.1088/1475-7516/2013/04/013.
- [15] Doyoun Kim, Peter Athron, Csaba Balázs, Benjamin Farmer, and Elliot Hutchison. Bayesian naturalness of the CMSSM and CNMSSM. *Phys. Rev.*, D90(5):055008, 2014. doi: 10.1103/PhysRevD.90.055008.
- [16] O. Buchmueller et al. The CMSSM and NUHM1 after LHC Run 1. *Eur. Phys. J.*, C74(6): 2922, 2014. doi: 10.1140/epjc/s10052-014-2922-3.
- [17] Leszek Roszkowski, Enrico Maria Sessolo, and Andrew J. Williams. What next for the CMSSM and the NUHM: Improved prospects for superpartner and dark matter detection. *JHEP*, 08:067, 2014. doi: 10.1007/JHEP08(2014)067.
- [18] Philip Bechtle et al. Killing the cMSSM softly. *Eur. Phys. J.*, C76(2):96, 2016. doi: 10.1140/epjc/s10052-015-3864-0.
- [19] Q. R. Ahmad et al. Direct evidence for neutrino flavor transformation from neutral current interactions in the Sudbury Neutrino Observatory. *Phys. Rev. Lett.*, 89:011301, 2002. doi: 10.1103/PhysRevLett.89.011301.
- [20] Y. Fukuda et al. Evidence for oscillation of atmospheric neutrinos. *Phys. Rev. Lett.*, 81: 1562–1567, 1998. doi: 10.1103/PhysRevLett.81.1562.
- [21] M. H. Ahn et al. Indications of neutrino oscillation in a 250 km long baseline experiment. *Phys. Rev. Lett.*, 90:041801, 2003. doi: 10.1103/PhysRevLett.90.041801.
- [22] Chiara Arina and Nicolao Fornengo. Sneutrino cold dark matter, a new analysis: Relic abundance and detection rates. *JHEP*, 11:029, 2007. doi: 10.1088/1126-6708/2007/11/029.
- [23] Chiara Arina, Maria Eugenia Cabrera Catalan, Sabine Kraml, Suchita Kulkarni, and Ursula Laa. Constraints on sneutrino dark matter from LHC Run 1. *JHEP*, 05:142, 2015. doi: 10.1007/JHEP05(2015)142.
- [24] Mitsuru Kakizaki, Eun-Kyung Park, Jae-hyeon Park, and Akiteru Santa. Phenomenological constraints on light mixed sneutrino dark matter scenarios. *Phys. Lett.*, B749:44–49, 2015. doi: 10.1016/j.physletb.2015.07.030.
- [25] Beranger Dumont, Genevieve Belanger, Sylvain Fichet, Sabine Kraml, and Thomas Schwetz. Mixed sneutrino dark matter in light of the 2011 XENON and LHC results. *JCAP*, 1209:013, 2012. doi: 10.1088/1475-7516/2012/09/013.
- [26] Genevieve Belanger, Sabine Kraml, and Andre Lessa. Light Sneutrino Dark Matter at the LHC. *JHEP*, 07:083, 2011. doi: 10.1007/JHEP07(2011)083.
- [27] Chiara Arina and Maria Eugenia Cabrera. Multi-lepton signatures at LHC from sneutrino dark matter. *JHEP*, 04:100, 2014. doi: 10.1007/JHEP04(2014)100.
- [28] Zachary Thomas, David Tucker-Smith, and Neal Weiner. Mixed Sneutrinos, Dark Matter and the CERN LHC. *Phys. Rev.*, D77:115015, 2008. doi: 10.1103/PhysRevD.77.115015.

- [29] P. S. Bhupal Dev, Subhadeep Mondal, Biswarup Mukhopadhyaya, and Sourov Roy. Phenomenology of Light Sneutrino Dark Matter in cMSSM/mSUGRA with Inverse Seesaw. *JHEP*, 09:110, 2012. doi: 10.1007/JHEP09(2012)110.
- [30] Shankha Banerjee, P. S. Bhupal Dev, Subhadeep Mondal, Biswarup Mukhopadhyaya, and Sourov Roy. Invisible Higgs Decay in a Supersymmetric Inverse Seesaw Model with Light Sneutrino Dark Matter. *JHEP*, 10:221, 2013. doi: 10.1007/JHEP10(2013)221.
- [31] G. Bélanger, J. Da Silva, and A. Pukhov. The Right-handed sneutrino as thermal dark matter in U(1) extensions of the MSSM. *JCAP*, 1112:014, 2011. doi: 10.1088/1475-7516/2011/12/014.
- [32] G. Bélanger, J. Da Silva, U. Laa, and A. Pukhov. Probing U(1) extensions of the MSSM at the LHC Run I and in dark matter searches. *JHEP*, 09:151, 2015. doi: 10.1007/JHEP09(2015)151.
- [33] David G. Cerdeno and Osamu Seto. Right-handed sneutrino dark matter in the NMSSM. *JCAP*, 0908:032, 2009. doi: 10.1088/1475-7516/2009/08/032.
- [34] Jonathan L. Feng, Arvind Rajaraman, and Fumihiro Takayama. Superweakly interacting massive particles. *Phys. Rev. Lett.*, 91:011302, 2003. doi: 10.1103/PhysRevLett.91.011302.
- [35] Jonathan L. Feng, Shufang Su, and Fumihiro Takayama. Supergravity with a gravitino LSP. *Phys. Rev.*, D70:075019, 2004. doi: 10.1103/PhysRevD.70.075019.
- [36] John R. Ellis, Keith A. Olive, Yudi Santoso, and Vassilis C. Spanos. Gravitino dark matter in the CMSSM. *Phys. Lett.*, B588:7–16, 2004. doi: 10.1016/j.physletb.2004.03.021.
- [37] Howard Baer, Ki-Young Choi, Jihn E. Kim, and Leszek Roszkowski. Dark matter production in the early Universe: beyond the thermal WIMP paradigm. *Phys. Rept.*, 555: 1–60, 2015. doi: 10.1016/j.physrep.2014.10.002.
- [38] Sudhir Kumar Gupta, Biswarup Mukhopadhyaya, and Santosh Kumar Rai. Right-chiral sneutrinos and long-lived staus: Event characteristics at the large hadron collider. *Phys. Rev.*, D75:075007, 2007. doi: 10.1103/PhysRevD.75.075007.
- [39] Sanjoy Biswas and Biswarup Mukhopadhyaya. Chargino reconstruction in supersymmetry with long-lived staus. *Phys. Rev.*, D81:015003, 2010. doi: 10.1103/PhysRevD.81.015003.
- [40] Sanjoy Biswas and Biswarup Mukhopadhyaya. Neutralino reconstruction in supersymmetry with long-lived staus. *Phys. Rev.*, D79:115009, 2009. doi: 10.1103/PhysRevD.79.115009.
- [41] Jan Heisig and Jörn Kersten. Production of long-lived staus in the Drell-Yan process. *Phys. Rev.*, D84:115009, 2011. doi: 10.1103/PhysRevD.84.115009.
- [42] Jan Heisig and Jörn Kersten. Long-lived staus from strong production in a simplified model approach. *Phys. Rev.*, D86:055020, 2012. doi: 10.1103/PhysRevD.86.055020.
- [43] Jan Heisig, Andre Lessa, and Loic Quertenmont. Simplified Models for Exotic BSM Searches. *JHEP*, 12:087, 2015. doi: 10.1007/JHEP12(2015)087.
- [44] Jan Heisig, Jörn Kersten, Boris Panes, and Tania Robens. A survey for low stau yields in the MSSM. *JHEP*, 04:053, 2014. doi: 10.1007/JHEP04(2014)053.
- [45] Koji Ishiwata, Masahiro Kawasaki, Kazunori Kohri, and Takeo Moroi. Right-handed sneutrino dark matter and big-bang nucleosynthesis. *Phys. Lett.*, B689:163–168, 2010. doi: 10.1016/j.physletb.2010.04.054.

- [46] F. Capozzi, G. L. Fogli, E. Lisi, A. Marrone, D. Montanino, and A. Palazzo. Status of three-neutrino oscillation parameters, circa 2013. *Phys. Rev.*, D89:093018, 2014. doi: 10.1103/PhysRevD.89.093018.
- [47] Antonio J. Cuesta, Viviana Niro, and Licia Verde. Neutrino mass limits: robust information from the power spectrum of galaxy surveys. 2015.
- [48] Takehiko Asaka, Koji Ishiwata, and Takeo Moroi. Right-handed sneutrino as cold dark matter. *Phys. Rev.*, D73:051301, 2006. doi: 10.1103/PhysRevD.73.051301.
- [49] Stephen P. Martin. A Supersymmetry primer. 1997. doi: 10.1142/9789812839657_0001, 10.1142/9789814307505_0001. [Adv. Ser. Direct. High Energy Phys.18,1(1998)].
- [50] Graham D. Kribs, Adam Martin, and Tuhin S. Roy. Supersymmetry with a Chargino NLSP and Gravitino LSP. *JHEP*, 01:023, 2009. doi: 10.1088/1126-6708/2009/01/023.
- [51] Takehiko Asaka, Koji Ishiwata, and Takeo Moroi. Right-handed sneutrino as cold dark matter of the universe. *Phys. Rev.*, D75:065001, 2007. doi: 10.1103/PhysRevD.75.065001.
- [52] G. Bélanger, F. Boudjema, A. Pukhov, and A. Semenov. MicrOMEGAs: A Program for calculating the relic density in the MSSM. *Comput. Phys. Commun.*, 149:103–120, 2002. doi: 10.1016/S0010-4655(02)00596-9.
- [53] G. Bélanger, F. Boudjema, A. Pukhov, and A. Semenov. micrOMEGAs4.1: two dark matter candidates. *Comput. Phys. Commun.*, 192:322–329, 2015. doi: 10.1016/j.cpc.2015.03.003.
- [54] Werner Porod. SPheno, a program for calculating supersymmetric spectra, SUSY particle decays and SUSY particle production at e+ e- colliders. *Comput. Phys. Commun.*, 153: 275–315, 2003. doi: 10.1016/S0010-4655(03)00222-4.
- [55] W. Porod and F. Staub. SPheno 3.1: Extensions including flavour, CP-phases and models beyond the MSSM. *Comput. Phys. Commun.*, 183:2458–2469, 2012. doi: 10.1016/j.cpc.2012.05.021.
- [56] Georges Aad et al. Combined Measurement of the Higgs Boson Mass in pp Collisions at $\sqrt{s} = 7$ and 8 TeV with the ATLAS and CMS Experiments. *Phys. Rev. Lett.*, 114:191803, 2015. doi: 10.1103/PhysRevLett.114.191803.
- [57] Georges Aad et al. Measurements of the Higgs boson production and decay rates and coupling strengths using pp collision data at $\sqrt{s} = 7$ and 8 TeV in the ATLAS experiment. *Eur. Phys. J.*, C76(1):6, 2016. doi: 10.1140/epjc/s10052-015-3769-y.
- [58] Vardan Khachatryan et al. Precise determination of the mass of the Higgs boson and tests of compatibility of its couplings with the standard model predictions using proton collisions at 7 and 8 TeV. *Eur. Phys. J.*, C75(5):212, 2015. doi: 10.1140/epjc/s10052-015-3351-7.
- [59] Jeremy Bernon and Beranger Dumont. Lilith: a tool for constraining new physics from Higgs measurements. *Eur. Phys. J.*, C75(9):440, 2015. doi: 10.1140/epjc/s10052-015-3645-9.
- [60] CMS Collaboration. Searches for Long-lived Charged Particles in Proton-Proton Collisions at $\sqrt{s} = 13$ TeV. Technical Report CMS-PAS-EXO-15-010, CERN, Geneva, 2015. URL <https://cds.cern.ch/record/2114818>.
- [61] Serguei Chatrchyan et al. Searches for long-lived charged particles in pp collisions at $\sqrt{s}=7$ and 8 TeV. *JHEP*, 07:122, 2013. doi: 10.1007/JHEP07(2013)122.

- [62] Georges Aad et al. Searches for heavy long-lived charged particles with the ATLAS detector in proton-proton collisions at $\sqrt{s} = 8$ TeV. *JHEP*, 01:068, 2015. doi: 10.1007/JHEP01(2015)068.
- [63] Heavy Flavor Averaging Group. 2013. URL www.slac.stanford.edu/xorg/hfag/rare/2013/rad11/btosg.pdf.
- [64] Vardan Khachatryan et al. Observation of the rare $B_s^0 \rightarrow \mu^+ \mu^-$ decay from the combined analysis of CMS and LHCb data. *Nature*, 2015. doi: 10.1038/nature14474.
- [65] Heavy Flavor Averaging Group. 2013. URL www.slac.stanford.edu/xorg/hfag/rare/2013/rad11/OUTPUT/HTML/rad11_table7.html.
- [66] ATLAS Collaboration. Search for pair-production of gluinos decaying via stop and sbottom in events with b -jets and large missing transverse momentum in $\sqrt{s} = 13$ TeV pp collisions with the ATLAS detector. Technical Report ATLAS-CONF-2015-067, CERN, Geneva, Dec 2015. URL <https://cds.cern.ch/record/2114839>.
- [67] Georges Aad et al. Summary of the searches for squarks and gluinos using $\sqrt{s} = 8$ TeV pp collisions with the ATLAS experiment at the LHC. *JHEP*, 10:054, 2015. doi: 10.1007/JHEP10(2015)054.
- [68] Fabio Iocco, Gianpiero Mangano, Gennaro Miele, Ofelia Pisanti, and Pasquale D. Serpico. Primordial Nucleosynthesis: from precision cosmology to fundamental physics. *Phys. Rept.*, 472:1–76, 2009. doi: 10.1016/j.physrep.2009.02.002.
- [69] Richard H. Cyburt, Brian D. Fields, Keith A. Olive, and Tsung-Han Yeh. Big Bang Nucleosynthesis: 2015. 2015.
- [70] Vivian Poulin and Pasquale D. Serpico. Loophole to the Universal Photon Spectrum in Electromagnetic Cascades and Application to the Cosmological Lithium Problem. *Phys. Rev. Lett.*, 114(9):091101, 2015. doi: 10.1103/PhysRevLett.114.091101.
- [71] Vivian Poulin and Pasquale Dario Serpico. Nonuniversal BBN bounds on electromagnetically decaying particles. *Phys. Rev.*, D91(10):103007, 2015. doi: 10.1103/PhysRevD.91.103007.
- [72] Masahiro Kawasaki, Kazunori Kohri, and Takeo Moroi. Big-Bang nucleosynthesis and hadronic decay of long-lived massive particles. *Phys. Rev.*, D71:083502, 2005. doi: 10.1103/PhysRevD.71.083502.
- [73] Karsten Jedamzik. Big bang nucleosynthesis constraints on hadronically and electromagnetically decaying relic neutral particles. *Phys. Rev.*, D74:103509, 2006. doi: 10.1103/PhysRevD.74.103509.
- [74] O. Pisanti, A. Cirillo, S. Esposito, F. Iocco, G. Mangano, G. Miele, and P. D. Serpico. PArthENoPE: Public Algorithm Evaluating the Nucleosynthesis of Primordial Elements. *Comput. Phys. Commun.*, 178:956–971, 2008. doi: 10.1016/j.cpc.2008.02.015.
- [75] Lawrence Kawano. Let’s go: Early universe. 2. Primordial nucleosynthesis: The Computer way. 1992.
- [76] Y. I. Izotov and T. X. Thuan. Systematic effects and a new determination of the primordial abundance of He-4 and dY/dZ from observations of blue compact galaxies. *Astrophys. J.*, 602:200–230, 2004. doi: 10.1086/380830.
- [77] David Kirkman, David Tytler, Nao Suzuki, John M. O’Meara, and Dan Lubin. The Cosmological baryon density from the deuterium to hydrogen ratio towards QSO

- absorption systems: D/H towards Q1243+3047. *Astrophys. J. Suppl.*, 149:1, 2003. doi: 10.1086/378152.
- [78] K. A. Olive, P. Petitjean, E. Vangioni, and J. Silk. Higher D or Li: probes of physics beyond the standard model. *mnras*, 426:1427–1435, October 2012. doi: 10.1111/j.1365-2966.2012.21703.x.
 - [79] Ryan Cooke, Max Pettini, Regina A. Jorgenson, Michael T. Murphy, and Charles C. Steidel. Precision measures of the primordial abundance of deuterium. *Astrophys. J.*, 781(1):31, 2014. doi: 10.1088/0004-637X/781/1/31.
 - [80] N. Baro, F. Boudjema, and A. Semenov. Full one-loop corrections to the relic density in the MSSM: A Few examples. *Phys. Lett.*, B660:550–560, 2008. doi: 10.1016/j.physletb.2008.01.031.
 - [81] Manuel Drees and X. Tata. Signals for heavy exotics at hadron colliders and supercolliders. *Phys. Lett.*, B252:695–702, 1990. doi: 10.1016/0370-2693(90)90508-4.
 - [82] Aleandro Nisati, Silvano Petrarca, and Giorgio Salvini. On the possible detection of massive stable exotic particles at the LHC. *Mod. Phys. Lett.*, A12:2213–2222, 1997. doi: 10.1142/S0217732397002260.
 - [83] Stephen P. Martin and James D. Wells. Cornering gauge mediated supersymmetry breaking with quasistable sleptons at the Tevatron. *Phys. Rev.*, D59:035008, 1999. doi: 10.1103/PhysRevD.59.035008.
 - [84] Jonathan L. Feng and Takeo Moroi. Supernatural supersymmetry: Phenomenological implications of anomaly mediated supersymmetry breaking. *Phys. Rev.*, D61:095004, 2000. doi: 10.1103/PhysRevD.61.095004.
 - [85] S. Ambrosanio, B. Mele, S. Petrarca, G. Polesello, and A. Rimoldi. Measuring the SUSY breaking scale at the LHC in the slepton NLSP scenario of GMSB models. *JHEP*, 01:014, 2001. doi: 10.1088/1126-6708/2001/01/014.
 - [86] Wilfried Buchmuller, Koichi Hamaguchi, Michael Ratz, and Tsutomu Yanagida. Supergravity at colliders. *Phys. Lett.*, B588:90–98, 2004. doi: 10.1016/j.physletb.2004.03.016.
 - [87] John R. Ellis, Are R. Raklev, and Ola K. Oye. Gravitino dark matter scenarios with massive metastable charged sparticles at the LHC. *JHEP*, 10:061, 2006. doi: 10.1088/1126-6708/2006/10/061.
 - [88] I. Hinchliffe and F. E. Paige. Measurements in gauge mediated SUSY breaking models at CERN LHC. *Phys. Rev.*, D60:095002, 1999. doi: 10.1103/PhysRevD.60.095002.
 - [89] Peter Z. Skands et al. SUSY Les Houches accord: Interfacing SUSY spectrum calculators, decay packages, and event generators. *JHEP*, 07:036, 2004. doi: 10.1088/1126-6708/2004/07/036.
 - [90] J. Alwall, R. Frederix, S. Frixione, V. Hirschi, F. Maltoni, O. Mattelaer, H. S. Shao, T. Stelzer, P. Torrielli, and M. Zaro. The automated computation of tree-level and next-to-leading order differential cross sections, and their matching to parton shower simulations. *JHEP*, 07:079, 2014. doi: 10.1007/JHEP07(2014)079.
 - [91] Torbjorn Sjostrand, Stephen Mrenna, and Peter Z. Skands. PYTHIA 6.4 Physics and Manual. *JHEP*, 05:026, 2006. doi: 10.1088/1126-6708/2006/05/026.

- [92] J. de Favereau, C. Delaere, P. Demin, A. Giammanco, V. Lemaître, A. Mertens, and M. Selvaggi. DELPHES 3, A modular framework for fast simulation of a generic collider experiment. *JHEP*, 02:057, 2014. doi: 10.1007/JHEP02(2014)057.
- [93] J. Pumplin, D. R. Stump, J. Huston, H. L. Lai, Pavel M. Nadolsky, and W. K. Tung. New generation of parton distributions with uncertainties from global QCD analysis. *JHEP*, 07: 012, 2002. doi: 10.1088/1126-6708/2002/07/012.
- [94] Matteo Cacciari, Gavin P. Salam, and Gregory Soyez. The Anti-k(t) jet clustering algorithm. *JHEP*, 04:063, 2008. doi: 10.1088/1126-6708/2008/04/063.
- [95] Matteo Cacciari, Gavin P. Salam, and Gregory Soyez. FastJet User Manual. *Eur. Phys. J.*, C72:1896, 2012. doi: 10.1140/epjc/s10052-012-1896-2.
- [96] W. Beenakker, M. Klasen, M. Kramer, T. Plehn, M. Spira, and P. M. Zerwas. The Production of charginos / neutralinos and sleptons at hadron colliders. *Phys. Rev. Lett.*, 83: 3780–3783, 1999. doi: 10.1103/PhysRevLett.100.029901,10.1103/PhysRevLett.83.3780. [Erratum: *Phys. Rev. Lett.*100,029901(2008)].
- [97] Claudio Muselli, Marco Bonvini, Stefano Forte, Simone Marzani, and Giovanni Ridolfi. Top Quark Pair Production beyond NNLO. *JHEP*, 08:076, 2015. doi: 10.1007/JHEP08(2015)076.
- [98] Stefano Catani, Leandro Cieri, Giancarlo Ferrera, Daniel de Florian, and Massimiliano Grazzini. Vector boson production at hadron colliders: a fully exclusive QCD calculation at NNLO. *Phys. Rev. Lett.*, 103:082001, 2009. doi: 10.1103/PhysRevLett.103.082001.
- [99] Johan Alwall et al. Comparative study of various algorithms for the merging of parton showers and matrix elements in hadronic collisions. *Eur. Phys. J.*, C53:473–500, 2008. doi: 10.1140/epjc/s10052-007-0490-5.
- [100] John M. Campbell, R. Keith Ellis, and Ciaran Williams. Vector boson pair production at the LHC. *JHEP*, 07:018, 2011. doi: 10.1007/JHEP07(2011)018.
- [101] Jonas M. Lindert, Frank D. Steffen, and Maïke K. Trenkel. Direct stau production at hadron colliders in cosmologically motivated scenarios. *JHEP*, 08:151, 2011. doi: 10.1007/JHEP08(2011)151.
- [102] B. Acharya et al. The Physics Programme Of The MoEDAL Experiment At The LHC. *Int. J. Mod. Phys.*, A29:1430050, 2014. doi: 10.1142/S0217751X14300506.